Vertical Grid Shifting Approach to the Development of Contrail Reduction Strategies with Sector Capacity Constraints

Peng Wei * Banavar Sridhar † Neil Chen † Dengfeng Sun*

Many strategies have been proposed to reduce contrail formation in the United States airspace. One approach is to build three-dimensional weather grids and have aircraft cruising at different flight levels to avoid the persistent contrail potential area with the consideration to constraints like fuel burn, flight level capacity, and total operations of climbing/descending aircraft count at each level. However, there is no air traffic control regulation defining the flight level capacity and the total number of climbing/descending aircraft operations for each flight level. This paper presents a contrail reduction scheme, which considers the defined Monitor Alert Parameter value as the sector capacity constraint. Instead of shifting (changing cruise altitude among vertical grids) for all aircraft in a center, the new scheme only shifts certain aircraft out of those grids that are within the persistent contrail potential area. Compared with the level shifting scheme, the grid shifting has a finer resolution and brings the benefits of more contrail reduction and less fuel burn. Furthermore, the one-hour planning interval is changed to one-minute, which provides higher temporal resolution in solution results. Numerical experiments are performed to compare the new vertical grid shifting scheme with the previous level shifting scheme.

Nomenclature

T	temperature in Celsius
RHw	relative humidity with respect to water
RHi	relative humidity with respect to ice
t	planning interval
l	cruising altitude level index
R_t^l	potential persistent contrail formation matrix (contrail matrix) at time t at level l
A_t^l	aircraft position matrix at time t at level l
CFI	center contrail frequency index
S_m^l	sector identification matrix of the mth sector at level l
B_t^l	sector congestion matrix at time t at level l

I. Introduction

The visible trails of condensed water vapor made by the exhaust of aircraft engines are called contrails. Contrails may exist for only a few seconds or several minutes, or may persist for many hours which may affect climate. Persistent contrails reduce incoming solar radiation and outgoing thermal radiation in a way that accumulates heat.[1] The global mean contrail cover in 1992 was estimated to double by 2015, and quadruple by 2050 due to air traffic increase.[2] Studies suggest that the environmental impact from persistent contrail is estimated to be three or four times,[3] to ten times[4] larger than aviation-induced emissions like CO_2 and NO_x. Therefore, strategies and policies to reduce aircraft induced persistent contrails need to be studied to minimize the impact on the global environment.

---

*School of Aeronautics and Astronautics, Purdue University
†NASA Ames Research Center, Moffett Field, CA

American Institute of Aeronautics and Astronautics

Several researchers have studied how to identify and reduce persistent contrail formation. Gierens, Limb and Eleftheratos in Ref. 5 and Noppel and Singh in Ref. 6 reviewed various strategies for contrail avoidance including changing engine architecture, enhancing airframe and engine integration, using alternate fuels, and modifying traffic flow management procedures. Among the traffic flow management solutions, Mannstein, Spichtinger and Gierens[7] presented a strategy to reduce the environmental impact of contrails significantly by small changes to each aircraft's flight altitude. Campbell, Neogi and Bragg[8] proposed a mixed integer programming method to optimally reroute aircraft to avoid the formation of persistent contrails. Both methods require an onboard contrail detection system. Fichter, Marquart, Sausen and Lee[9] showed that the global annual mean contrail coverage could be reduced by decreasing the aircraft cruise altitude. Williams, Noland and Toumi[10, 11] proposed strategies for contrail reduction by identifying fixed and varying maximum altitude restrictions. These restrictions generally require more fuel burn and add congestion to the already crowded airspace at lower altitudes. Sridhar, Chen and Ng[12, 13] defined the contrail frequency index to model and predict persistent contrail formation. They provided a set of strategies to reduce contrail formation. A three-dimensional (3D) weather grid model was constructed to describe the contrail potential areas and the flight level of aircraft is adjusted to avoid these areas with the consideration of fuel burn trade-off. Chen, Sridhar, Li and Ng evaluated the contrail reduction strategies based on aircraft travel distances.[14] Sridhar, Ng and Chen integrated emission and climate models together with air traffic simulations to further understand the complex interaction between the physical climate system, emissions and air traffic.[15] They analyzed the trade-offs between extra fuel burn and reduction of global surface temperature change. Wei, Sridhar, Chen and Sun[16] continued the research on flight level shifting (changing cruise altitude) strategy considering the constraints of flight level capacity and climbing/descending aircraft operations limit introduced by air traffic controllers' operational feasibility. However, in practice, there is no air traffic control regulation on capacity or operations limit at each flight level. Instead, the Monitor Alert Parameter (MAP) value is assigned to each sector to limit the aircraft count and maintain a manageable number of operations for air traffic controllers. Evans, Chen, Sridhar and Ng[17] discussed the contrail reduction strategies and emissions under MAP value constraint, in which the sector counts were monitored by the Future Air traffic management Concepts Evaluation Tool (FACET).[18]

In this paper, the sector capacity limits (MAP values) were integrated into the 3D grid model. In addition, considering that shifting all the aircraft from their current cruising level to another level results in more fuel burn, the finer grid shifting scheme was developed to change aircraft cruise altitude in each grid.

In this work, the authors apply the MAP value to the 3D grid model in order to investigate the trade-off between contrail reduction and sector congestion. Shifting all the aircraft at one flight level[12, 16] is replaced to shifting them to different vertical grids, which will reduce the fuel burn. In order to obtain better temporal resolution, the one hour planning interval proposed in[12, 16] is changed to one minute. The new grid shifting scheme is developed with and without considering the sector capacity constraint. The simulation first compares the contrail reduction results of level shifting and free grid shifting without considering sector capacities. Then the performance of grid shifting satisfying sector capacity constraint is analyzed.

The rest of the paper is organized as follows. Section II introduces the atmospheric data, contrail formation model, aircraft data and contrail frequency index used in this paper. Section III presents the problem formulation with the higher temporal resolution model. The solution methodology of grid shifting is presented in Section IV. The numerical results are shown in Section V. Section VI summarizes and concludes the paper.

II.   Data and Model

A.   Atmospheric Data

Contrails can be observed from surface data[19] and detected by satellite data.[20] Duda, Palikonda and Minnis[21] have related the observations to numerical weather analysis output and showed that persistent contrail formation can be computed using atmospheric temperature and humidity data retrieved from the Rapid Updated Cycle (RUC) data provided by the National Oceanic and Atmospheric Administration (NOAA). Contrails can persist when ambient air is supersaturated with respect to ice, which means that relative humidity with respect to ice (RHi) is greater than one hundred percent.[22] The RHi can be computed from relative humidity with respect to water (RHw) and temperature, which are available in the RUC data. The one-hour forecast and the 13-km RUC data are used in this paper. The data have a temporal resolution of one hour, a horizontal resolution of 13 kilometers, and isobaric pressure levels from 100 to 1000 hectopascals

American Institute of Aeronautics and Astronautics

(hPa) with 25 hPa increments. The vertical range of interest in this study is from 150 hPa to 400 hPa, which is equivalent to pressure altitude of about 23,600 feet to 44,400 feet.

The temperature and RHw contours at 8AM eastern daylight time (EDT) on August 1, 2007 at pressure altitude 250 hPa, or 34,057 feet, are shown as in Fig. 1.
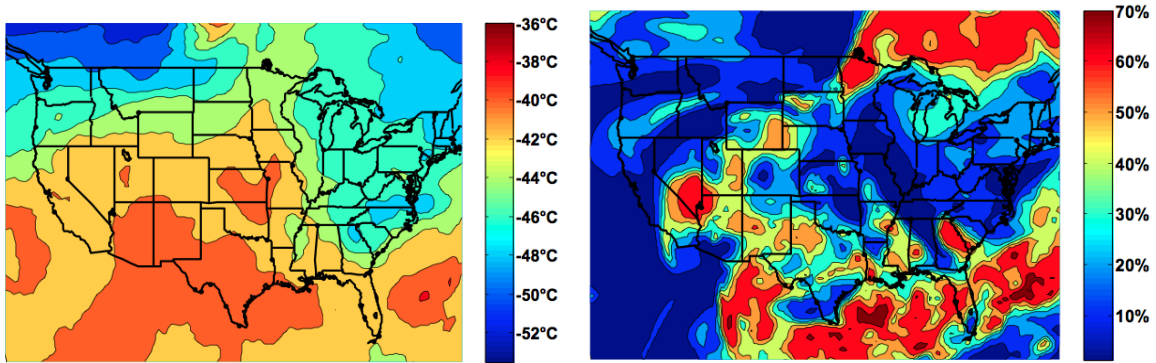
Figure 1.   Contours of temperature and RHw at 34,057 feet at 8AM EDT on August 1, 2007.

B.   Contrail Formation Model

The potential persistent contrail formation areas (contrail areas) are defined as areas with RHi greater than or equal to 100%. RHi can be computed from RHw and temperature using the saturation vapor pressure coefficients of Alduchov,[23] formulated as

$$RHi = RHw \times \frac{6.0612e^{18.102T/(249.52+T)}}{6.1162e^{22.577T/(237.78+T)}}, \tag{1}$$

where T is the temperature in Celsius. The atmospheric profile shown in the left and right subfigures in Fig. 1 can be translated to a contour of RHi, as shown in Fig. 2.
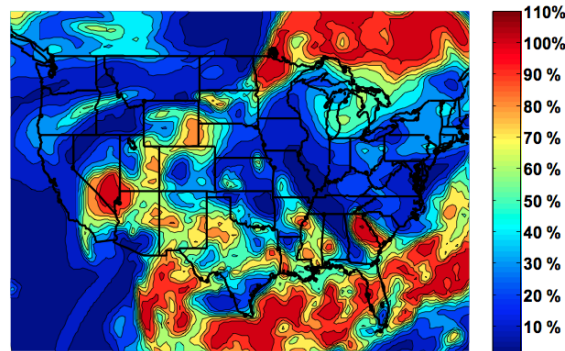
Figure 2.   Contour of RHi at 34,057 feet at 8AM EDT on August 1, 2007.

The 13-km RUC data have (337×451) data points that cover most U.S. airspace. The altitude level index l is defined as $l = 1, 2, ..., 11$ corresponding to isobaric pressure level at $400, 375, ..., 150$ hPa. The level index, isobaric pressure level, and approximate aircraft cruising altitude are listed in Table 1.

Table 1.   Level index, isobaric pressure level and approximate aircraft cruising altitude.

Level index	1	2	3	4	5	6	7	8	9	10	11
Pressure level (hPa)	400	375	350	325	300	275	250	225	200	175	150
Cruising altitude (100 feet)	236	251	267	283	301	320	341	363	387	414	444

American Institute of Aeronautics and Astronautics

The potential persistent contrail formation matrix (contrail matrix) at time t at level l is defined as

$$R_t^l = \begin{pmatrix} r_{1,1,l} & r_{1,2,l} & \cdots & r_{1,451,l} \\ \vdots & \vdots & \ddots & \vdots \\ r_{337,1,l} & r_{337,2,l} & \cdots & r_{337,451,l} \end{pmatrix}, \tag{2}$$

where $r_{i,j}$ is 1 if RHi $\geq 100\%$ at grid (i,j) and 0 if RHi $< 100\%$.

C. Aircraft Data

Contrail formation areas represent environmental conditions likely to produce contrails. Thus aircraft locations are needed to determine the contrail formation frequency. The aircraft data used in this paper are obtained from the aircraft locations provided by the Federal Aviation Administration's (FAA's) Aircraft Situation Display to Industry (ASDI) data. The ASDI has a sampling rate of one minute. The same 3D grid in the RUC data is used to generate the aircraft position matrix. The aircraft position matrix at level l is defined as

$$A_t^l = \begin{pmatrix} a_{1,1,l} & a_{1,2,l} & \cdots & a_{1,451,l} \\ \vdots & \vdots & \ddots & \vdots \\ a_{337,1,l} & a_{337,2,l} & \cdots & a_{337,451,l} \end{pmatrix}, \tag{3}$$

where $a_{i,j}$ is the number of aircraft within grid (i,j) flying closest to level l at time t. The aircraft position matrix indicates the air traffic density in the grid scale at different altitudes.

D. Contrail Frequency Index

The contrail frequency index (CFI) is defined as the number of aircraft that would fly through potential contrail formation regions during a period of time, and is used to indicate the contrail severity in a given region.[13]

The center contrail frequency index in center C_n is defined as the number of aircraft flying through persistent contrail potential area at time t within center C_n, formulated as

$$CFI_{C_n,t} = \sum_{i,j,l}^{C_n} r_{i,j,l} a_{i,j,l}, \tag{4}$$

where $r_{i,j,l}$ and $a_{i,j,l}$ are defined in Eqn. (2), (3).

The contrail frequency index indicates the actual contrail activities in a given region defined on a 3D grid. For strategic planning, the contrail frequency at time t of a certain center C_n is calculated by

$$CFI_{C_n,t} = \sum_{i,j,l}^{C_n} r'_{i,j,l} \hat{a}_{i,j,l}, \tag{5}$$

where $r'_{i,j,l}$ is from RUC forecast weather data and $\hat{a}_{i,j,l}$ is the predicted aircraft locations resulted from our optimal solutions. The goal of this work is to design an optimization method to decide $\hat{a}_{i,j,l}$'s such that the objective function $CFI_{C_n,t}$ is minimized under given constraints.

III. Problem

In this work the 3D grid is used for not only modeling the RUC weather data but also for shifting aircraft position vertically by grid. Two constraints are considered. The aircraft performance constraint requires that aircraft position can only be shifted up or down by one grid. Sector capacity constraint is introduced to maintain the manageable aircraft amount inside each sector for air traffic controllers. In summary, the grid shifting scheme is formulated as a linear programming problem.

American Institute of Aeronautics and Astronautics

A. Aircraft Performance Constraint

According to Base of Aircraft Data (BADA) by EUROCONTROL,[24] most of the typical climb/descent rates of en route commercial aircraft are less than 3,000 feet per minute, which indicates that we can only shift aircraft up or down by one grid during one minute because based on Table 1, each level varies from 1,500 to 3,000 feet.

For the $a_{i,j,l}$ aircraft used to cruise in grid (i,j,l), three variables $x_{i,j}^{l,l}$, $x_{i,j}^{l,l-1}$ and $x_{i,j}^{l,l+1}$ are adopted to denote how many aircraft will stay in current grid, descend to a lower altitude grid and climb to a higher altitude grid. Notice that for the grids at level 1 or level 11 (see in Table 1), there will be only $x_{i,j}^{l,l}$ and $x_{i,j}^{l,l+1}$ or $x_{i,j}^{l,l}$ and $x_{i,j}^{l,l-1}$.

$$a_{i,j,l} = \begin{cases} x_{i,j}^{l,l} + x_{i,j}^{l,l+1} & l = 1, \\ x_{i,j}^{l,l} + x_{i,j}^{l,l-1} & l = 11, \\ x_{i,j}^{l,l} + x_{i,j}^{l,l-1} + x_{i,j}^{l,l+1} & \text{otherwise.} \end{cases} \tag{6}$$

Similarly, the solution $\hat{a}_{i,j,l}$ consists of $x_{i,j}^{l,l}$, $x_{i,j}^{l-1,l}$ and $x_{i,j}^{l+1,l}$ except the grids at level 1 or level 11 which only consists of $x_{i,j}^{l,l}$ and $x_{i,j}^{l+1,l}$ or $x_{i,j}^{l,l}$ and $x_{i,j}^{l-1,l}$.

$$\hat{a}_{i,j,l} = \begin{cases} x_{i,j}^{l,l} + x_{i,j}^{l+1,l} & l = 1, \\ x_{i,j}^{l,l} + x_{i,j}^{l-1,l} & l = 11, \\ x_{i,j}^{l,l} + x_{i,j}^{l-1,l} + x_{i,j}^{l+1,l} & \text{otherwise.} \end{cases} \tag{7}$$

B. Sector Capacity Constraint

The Monitor Alert Parameter (MAP) value[25] is used as an indicator of a capacity limit for each sector of airspace. A sector's MAP value reflects the maximum aircraft count that can be safely handled by a sector controller. MAP values are set up as sector capacities in this work.

In order to impose a MAP value to a sector, we need to identify the sector in the 3D grid model described in Section II. The 3D sector identification matrix S_m is used to locate the grids inside the corresponding sector.

$$S_m^l = \begin{pmatrix} s_{1,1,l} & s_{1,2,l} & \cdots & s_{1,451,l} \\ \vdots & \vdots & \ddots & \vdots \\ s_{337,1,l} & s_{337,2,l} & \cdots & s_{337,451,l} \end{pmatrix}, \tag{8}$$

$s_{i,j,l} = 1$ if grid (i,j,l) is inside sector S_m and $s_{i,j,l} = 0$ otherwise. Thus the sector capacity constraint for sector m can be formulated as:

$$\sum_{i,j,l}^{337,451,11} s_{i,j,l}\hat{a}_{i,j,l} \leq \text{MAP}_m. \tag{9}$$

In short, Eqn. (9) for sector S_m can be written as:

$$\sum_{i,j,l}^{S_m} \hat{a}_{i,j,l} \leq \text{MAP}_m. \tag{10}$$

Similarly, the 3D center identify matrix is defined to locate all the grids in center C_n, in which the element $c_{i,j,l} = 1$ if grid (i,j,l) is inside center C_n and $s_{i,j,l} = 0$ otherwise. In this work, the contrail reduction scheme is applied within each center. Thus the objective function is to minimize the total contrail frequency index inside a certain center:

$$\min \sum_{i,j,l}^{337,451,11} c_{i,j,l} r'_{i,j,l} \hat{a}_{i,j,l} \tag{11}$$

In short, Eqn. (11) can be written as:

$$\min \sum_{i,j,l}^{C_n} r'_{i,j,l}\hat{a}_{i,j,l} = \min \sum_{i,j,l}^{C_n} CFI_{i,j,l} \tag{12}$$

American Institute of Aeronautics and Astronautics

C.   Problem Formulation

We consider the optimization problem inside one center within time interval t. $r'_{i,j,l}$'s are obtained from the weather forecast. The problem formulation is

$$\min \sum_{i,j,l}^{C_n} \text{CFI}_{i,j,l}$$
$$\text{s.t.} \quad (6), (7),$$
$$\sum_{i,j,l}^{S_m} \hat{a}_{i,j,l} \leq \text{MAP}_m, \forall S_m \in C_n. \tag{13}$$

i, j, l are the index for each 3D grid. $\text{CFI}_{i,j,l}$'s are the CFI number generated by the aircraft in grid (i, j, l) in t. C_n is the nth center. $a_{i,j,l}$ is the number of aircraft which used to cruise inside grid (i, j, l) in t. S_m is the mth sector in center C_n. MAP_m is the MAP value assigned to S_m.

IV.   Method

The grid shifting scheme is developed in this section, which provides better contrail reduction performance and less fuel burn than the level shifting scheme.

A.   Level Shifting vs. Grid Shifting

The level shifting scheme and grid shifting scheme are demonstrated in the left and right subfigures of Fig. 3. The blue aircraft are the positions before shifting and the black aircraft are the positions after shifting.
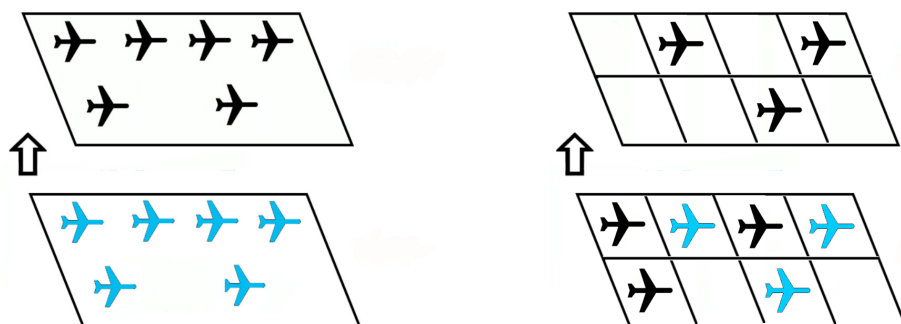
Figure 3.   Comparison between level shifting scheme and grid shifting scheme.

In the left subfigure, the level shifting moves all the aircraft at level l to level $l + 1$ when it finds that cruising at level $l + 1$ generates fewer CFI in total. In the right subfigure, the grid shifting only moves those aircraft that produce fewer CFI at level $l + 1$ than at l. Therefore the grid shifting is more accurate, and is expected to provide better contrail reduction results and less fuel burn. Furthermore, sector capacity constraints can be integrated into grid shifting.

B.   Grid Shifting Without Sector Capacity Constraint

Although the optimization problem in (13) is solvable by linear programming techniques, we can find solutions faster based on the special structure of the problem. We first introduce the free grid shifting scheme without considering sector capacity constraint. Then the grid shifting satisfying sector capacity constraint is proposed.

To develop the free grid shifting, the aircraft performance constraint still needs to be satisfied, which means that the aircraft can be only moved up or down by one flight level. We first observed that without the sector capacity constraint, all shifting moves for aircraft inside a grid are decoupled. By ignoring the sector capacity constraint, all the local optimal solutions for each grid together provide the global optimal

American Institute of Aeronautics and Astronautics

solution. The summation of all the local optimal solutions $\text{CFI}_{i,j,l}$ is the global optimal solution. Because

$$\sum_{i,j,l}^{C_n} \min \text{CFI}_{i,j,l} = \min \sum_{i,j,l}^{C_n} \text{CFI}_{i,j,l}$$

when there is no coupling sector capacity constraint among different grids.

The local optimal solution is easy to find by the greedy method. Consider the coefficient in objective function (12) is $r'_{i,j,l}$ which is either 1 or 0. Thus the idea is to check every grid and its upper and lower neighboring grids (grids at level 1 and level 11 only need to check one neighboring grid). If $r'_{i,j,l} = 0$ in this grid, there is no contrail formed and none of the aircraft in this grid need to be shifted. If $r'_{i,j,l} = 1$ in this grid, all the aircraft $a_{i,j,l}$ will produce persistent contrail. Now the potential persistent contrail formation values in its upper grid $r'_{i,j,l+1}$ and in its lower grid $r'_{i,j,l-1}$ are checked. If there is one of them equal to 0, we can avoid producing contrail in grid (i,j,l) by shifting $a_{i,j,l}$ to the corresponding neighboring grid. If both potential persistent contrail formation values of the neighboring grids are 0, shift all $a_{i,j,l}$ aircraft to the lower grid (or the upper grid). If $r'_{i,j,l} = 1$ in grid (i,j,l) and both potential persistent contrail formation values of its neighboring grids are 1, there is no contrail reduction shifting that can be performed.

The greedy algorithm is summarized in Algorithm 1:

Algorithm 1 Greedy Grid Shifting Algorithm

1: **for** i, j, l **do**
2:   **if** $r'_{i,j,l} == 1$ **then**
3:     **if** $r'_{i,j,l-1} == 0$ **then**
4:       shift to lower grid: $\hat{a}_{i,j,l} = 0$, $\hat{a}_{i,j,l-1} = a_{i,j,l-1} + a_{i,j,l}$
5:       continue
6:     **end if**
7:     **if** $r'_{i,j,l+1} == 0$ **then**
8:       shift to upper grid: $\hat{a}_{i,j,l} = 0$, $\hat{a}_{i,j,l+1} = a_{i,j,l+1} + a_{i,j,l}$
9:     **end if**
10:   **end if**
11: **end for**

C. Grid Shifting With Sector Capacity Constraint

An En Route Center is divided into smaller regions, called sectors, which can be further defined as low altitude sectors, high altitude sectors and super high altitude sectors. Each sector is monitored and controlled by at least one air traffic controller. In this work, high and super high sectors are considered by grid shifting because they can cover all 11 levels from 23,600 to 44,400 feet.

1. Identify the Congested Sectors

In order not to introduce extra congestion to a busy sector, we need to first identify the busy sector. A sector is called busy if the total aircraft count in this sector is larger than the assigned MAP value.

$$\sum_{i,j,l}^{337,451,11} s_{i,j,l} a_{i,j,l} > \text{MAP}_m.$$

The sector congestion matrix at time t at level l is defined as:

$$B_t^l = \begin{pmatrix} b_{1,1,l} & b_{1,2,l} & \ldots & b_{1,451,l} \\ \vdots & \vdots & \ddots & \vdots \\ b_{337,1,l} & b_{337,2,l} & \ldots & b_{337,451,l} \end{pmatrix}, \tag{14}$$

where $b_{i,j,l} = 1$ if grid (i,j,l) belongs to a busy sector and $b_{i,j,l} = 0$ otherwise.

American Institute of Aeronautics and Astronautics

2. Grid Shifting With Sector Capacity Constraint

Our target is to balance the contrail reduction and sector congestion. Therefore we want to design a scheme that will not introduce extra congestion to those already busy sectors.

Therefore, for grid (i, j, l) the first step is to check the value of the contrail formation coefficient $r'_{i,j,l}$. If $r'_{i,j,l} = 0$, no persistent contrail will be formed in current grid so contrail reduction shifting is not needed. If the contrail formation coefficient $r_{i,j,l} = 1$, its neighboring vertical grids are checked. When one of the upper and lower grids has the contrail formation coefficient equal to 0, which means moving a number of $a_{i,j,l}$ aircraft to this neighboring grid can reduce the total CFI by $a_{i,j,l}$, check the corresponding sector congestion value $b_{i,j,l}$. If $b_{i,j,l} = 0$, the neighboring grid is in a non-congested sector. The aircraft will be shifted. Otherwise, if $b_{i,j,l} = 1$, the neighboring grid is in a busy sector. The shifting move will not be performed. If $r'_{i,j,l} = 1$ and both of its neighboring grids have 0 contrail formation coefficient, the aircraft in grid (i, j, l) will be shifted to the grid with $b_{i,j,l} = 0$. If $r'_{i,j,l} = 1$ and both of its neighboring grids have contrail formation coefficient equal to 1, no shifting needs to be performed. The grid shifting scheme is fast and the contrail reduction computation for twenty U.S. centers in a day can be done in minutes.

The corresponding flow chart is illustrated in Fig. 4.
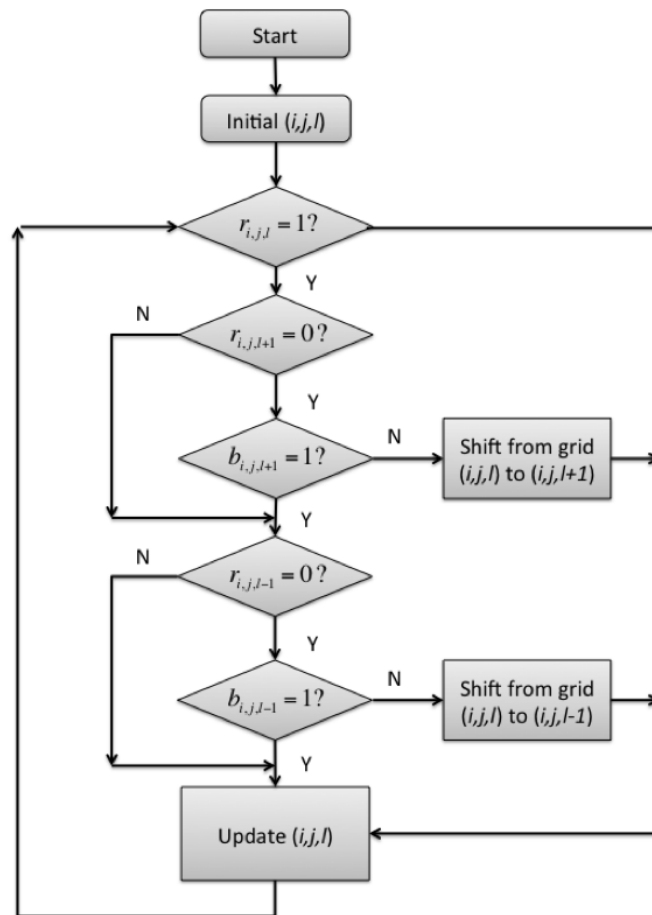
Figure 4. Flow chart of the grid shifting with sector capacity constraint.

The complete algorithm is listed in Algorithm 2:

American Institute of Aeronautics and Astronautics

Algorithm 2 Grid Shifting With Sector Capacity Constraint

1: **for** i, j, l **do**
2:    **if** $r'_{i,j,l} == 1$ **then**
3:       **if** $r'_{i,j,l+1} == 0$ **then**
4:          **if** $b_{i,j,l+1} == 0$ **then**
5:             shift to upper grid: $\hat{a}_{i,j,l} = 0$, $\hat{a}_{i,j,l+1} = a_{i,j,l+1} + a_{i,j,l}$
6:             continue
7:          **end if**
8:       **end if**
9:       **if** $r'_{i,j,l-1} == 0$ **then**
10:         **if** $b_{i,j,l-1} == 0$ **then**
11:            shift to lower grid: $\hat{a}_{i,j,l} = 0$, $\hat{a}_{i,j,l-1} = a_{i,j,l-1} + a_{i,j,l}$
12:         **end if**
13:       **end if**
14:    **end if**
15: **end for**

V. Results

The RUC weather data and the ASDI air traffic data on April 23, 2010 are used to build the 3D grid model. The high and super high sectors of twenty U.S. centers between flight level 1 and flight level 11 are considered for sector capacity constraint. 24 hours contrail reduction results are shown.

A. Contrail Reduction by Level Shifting and Free Grid Shifting

In Fig. 5 contrail frequency index results are listed for twenty U.S. centers. The blue bars are the contrail frequency indices without any contrail reduction strategy calculated from historical weather and air traffic data. Due to the different weather conditions and air traffic, 20 centers have various CFIs. We can see that on that particular day, Minneapolis center (ZMP) has the highest contrail frequency index, which is over 20,000. Also, the contrail frequency indices in Chicago Center (ZAU), Denver Center (ZDV) and Kansas City Center (ZKC) are higher than 5,000. New York Center (ZNY) has 0 CFI. Purple bars are the contrail frequency indices after the level shifting reduction method presented in [12]. To make a fair comparison, the +/- 1 level shifting method is implemented to compare with the +/- 1 grid shifting method. The green bars are the contrail frequency indices after the grid level shifting reduction method presented in Section IV. The results show that the level shifting method significantly reduces the CFI in ZMP by more than 50% and it provides more CFI reduction in ZAU, ZDV, ZKC and other centers. Moreover, the grid shifting method reduces the CFI in ZMP to about 33%, which is a larger reduction than level shifting method. Similarly, the grid shifting method achieves better CFI reduction than level shifting method in all U.S. 20 centers.
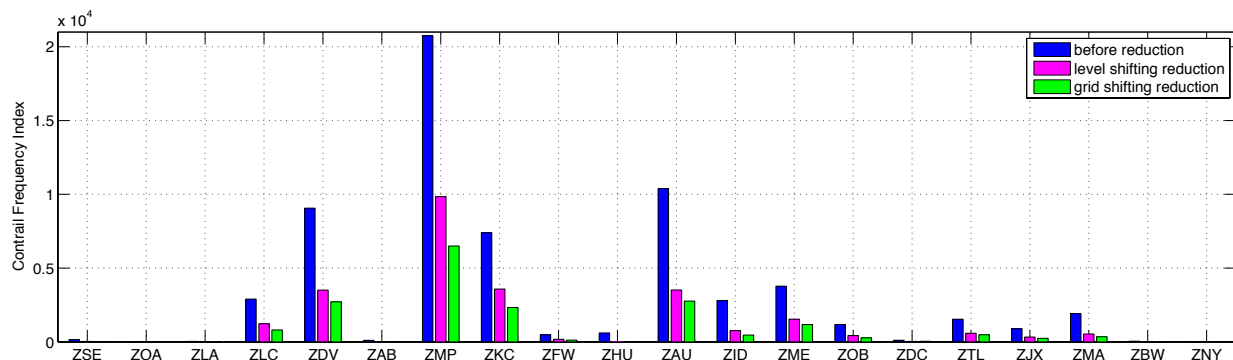
Figure 5. Comparison between level shifting scheme and grid shifting scheme.

American Institute of Aeronautics and Astronautics

B. Contrail Reduction by Free Grid Shifting and Grid Shifting With Sector Capacity Constraint

Fig. 6 shows that the contrail frequency index reduction comparison between the grid shifting method without sector capacity constraint and the grid shifting method with sector capacity constraint. The CFI reduction performances of the two methods are about the same. In other words, the grid shifting method satisfies the sector capacity constraint while achieving about the same amount of CFI reduction. In this way, no extra air traffic congestion will be introduced to each sector.
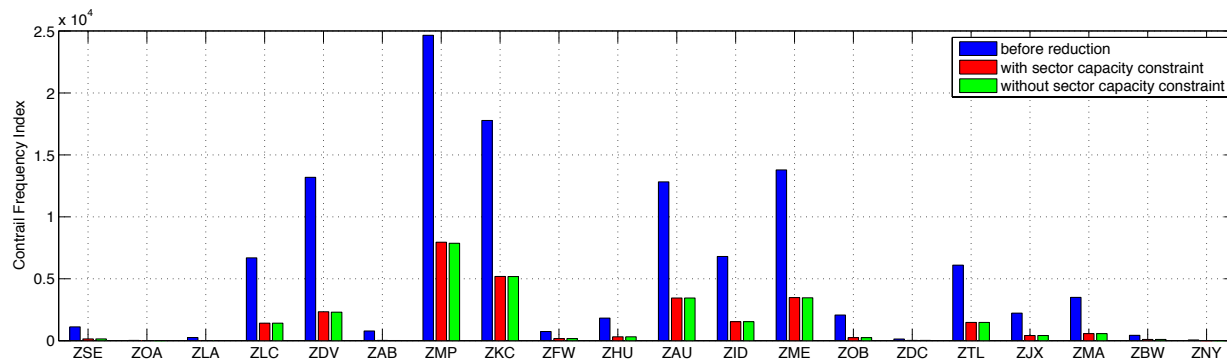
Figure 6. Comparison between grid shifting with sector capacity constraint and grid shifting without sector capacity constraint.

In detail, Table 2 lists the resulting CFIs of twenty centers after two types of grid shifting schemes. In most of the centers the grid shifting with sector capacity constraint has the close performance to the free grid shifting. However, in ZMP, the free shifting reduces CFI by about 100. The reason is that on the day of April 23, 2010, the potential contrail formation area overlaps with a busy sector in ZMP. To prevent introduce extra congestion into the busy sector, the grid shifting is not performed in the corresponding sector.

VI.   Conclusion

In this paper the grid shifting contrail reduction strategy was proposed. The one minute planning interval is adopted to have a higher temporal resolution than our previous work. The finer grid shifting algorithm can reduce more contrails than the level shifting method in all twenty U.S. centers in a day. Moreover, the grid shifting can identify the busy sectors and then balances the contrail reduction and sector congestion. The more accurate grid shifting brings the potential benefit of less fuel burn than level shifting scheme.

References

[1] Meerkotter, R., Schumann, U., Doelling, D., Minnis, P., Nakajima, T., and Tsushima, Y., "Radiative forcing by contrails," *Annales Geophysicae*, Vol. 17, 1999, pp. 1080–1094.

[2] Marquart, S., Ponater, M., Mager, F., and Sausen, R., "Future Development of Contrail Cover, Optical Depth and Radiative Forcing: Impacts of Increasing Air Traffic and Climate Change," *Journal of Climate*, Vol. 16, September 2003, pp. 2890–2904.

[3] "The Environmental Effects of Civil Aircraft in Flight," Tech. rep., Royal Commission on Environmental Pollution, London, UK, 2002.

[4] Mannstein, H. and Schumann, U., "Aircraft induced contrail cirrus over Europe," *Meteorologische Zeitschrift*, Vol. 14, No. 4, 2005, pp. 549–554.

[5] Gierens, K., Limb, L., and Eleftheratos, K., "A review of various strategies for contrail avoidance," *The Open Atmospheric Science Journal*, Vol. 2, 2008, pp. 1–7.

[6] Noppel, F. and Singh, R., "Overview on contrail and cirrus cloud avoidance technology," *Journal of Aircraft*, Vol. 44, No. 5, 2007, pp. 1721–1726.

[7] Mannstein, H., Spichtinger, P., and Gierens, K., "A note on how to avoid contrail cirrus," *Transportation Research. Part D, Transport and environment*, Vol. 10, No. 5, September 2005, pp. 421–426.

[8] Campbell, S. E., Neogi, N. A., and Bragg, M. B., "An optimal strategy for persistent contrail avoidance," *AIAA Guidance, Navigation and Control Conference*, AIAA, Honolulu, HI, August 2008.

American Institute of Aeronautics and Astronautics

Table 2. Contrail Frequency Indices of twenty U.S. centers after grid shifting with sector capacity constraint and without sector capacity constraint.

Centers	Shifting With Constraint	Free Shifting
ZSE	139	139
ZOA	6	0
ZLA	6	6
ZLC	1413	1413
ZDV	2334	2303
ZAB	18	16
ZMP	7950	7859
ZKC	5181	5179
ZFW	165	165
ZHU	312	312
ZAU	3442	3440
ZID	1531	1531
ZME	3474	3463
ZOB	239	239
ZDC	22	21
ZTL	1476	1469
ZJX	414	414
ZMA	569	569
ZBW	95	95
ZNY	0	0

[9]Fichter, C., Marquart, S., Sausen, R., and Lee, D. S., "The impact of cruise altitude on contrails and related radiative forcing," *Meteorologische Zeitschrift*, Vol. 14, No. 4, August 2005, pp. 563–572.

[10]Williams, V., Noland, R. B., and Toumi, R., "Reducing the climate change impacts of aviation by restricting cruise altitudes," *Transportation Research. Part D, Transport and environment*, Vol. 7, No. 5, November 2002, pp. 451–464.

[11]Williams, V. and Noland, R. B., "Variability of contrail formation conditions and the implications for policies to reduce the climate impacts of aviation," *Transportation Research. Part D, Transport and environment*, Vol. 10, No. 4, July 2005, pp. 269–280.

[12]Sridhar, B., Chen, N. Y., and Ng, H. K., "Fuel efficient strategies for reducing contrail formations in United States airspace," *AIAA Digital Avionics Systems Conference*, AIAA, Salt Lake City, UT, Oct 2010.

[13]Chen, N. Y., Sridhar, B., and Ng, H. K., "Prediction and use of contrail frequency index for contrail reduction strategies," *AIAA Guidance, Navigation and Control Conference*, AIAA, Toronto, Canada, Aug 2010.

[14]Chen, N. Y., Sridhar, B., Li, J., and Ng, H. K., "Evaluation of Contrail Reduction Strategies Based on Aircraft Flight Distances," *AIAA Guidance, Navigation and Control Conference*, Minneapolis, MN, Aug 2012.

[15]Sridhar, B., Ng, H. K., and Chen, N. Y., "Integration of Linear Dynamic Emission and Climate Models with Air Traffic Simulations," *AIAA Guidance, Navigation and Control Conference*, Minneapolis, MN, Aug 2012.

[16]Wei, P., Sridhar, B., Chen, N. Y., and Sun, D., "A Linear Programming Approach to the Development of Contrail Reduction Strategies Satisfying Operationally Feasible Constraints," *AIAA Guidance, Navigation and Control Conference*, Minneapolis, MN, Aug 2012.

[17]Evans, A., Chen, N. Y., Sridhar, B., and Ng, H. K., "Trade-off between Contrail Reduction and Emissions under Future US Air Traffic Scenarios," *AIAA Aviation Technology, Integration, and Operations Conference*, Indianapolis, Indiana, Sep 2012.

[18]Bilimoria, K., Sridhar, B., Chatterji, G., Sheth, K., and Grabbe, S., "FACET: Future ATM Concepts Evaluation Tool," *3rd USA/Europe Air Traffic Management Seminar*, Napoli, Italy, June 2000.

[19]Minnis, P., Ayers, J. K., Nordeen, M. L., and Weaver, S. P., "Contrail frequency over the united states from surface observations," *Journal of Climate*, Vol. 16, No. 21, November 2003.

[20]Palikonda, R., Minnis, P., Duda, D. P., and Mannstein, H., "Contrail coverage derived from 2001 AVHRR data over the continental United States of America and surrounding areas," *Meteorologische Zeitschrift*, Vol. 14, No. 4, August 2005, pp. 525–536.

[21]Duda, D. P., Palikonda, R., and Minnis, P., "Relating observations of contrail persistence to numerical weather analysis output," *Atmospheric Chemistry and Physics*, Vol. 9, No. 4, February 2009, pp. 1357–1364.

[22]Duda, D. P., Minnis, P., Costulis, P. K., and Palikonda, R., "Conus contrail frequency estimated from ruc and flight track

American Institute of Aeronautics and Astronautics

data," *European Conference on Aviation, Atmosphere, and Climate*, Friedrichshafen at Lake Constance, Germany, June-July 2003.

[23]Alduchov, O. A. and Eskridge, R. E., "Improved magnus form approximation of saturation vapor pressure," *Journal of Applied Meteorology*, Vol. 35, No. 4, April 1996, pp. 601–609.

[24]Eurocontrol Experimental Center (EEC), *User Manual for the Base of Aircraft Data (BADA), Revision 3.6*, Sep 2004, Note No. 10/04.

[25]*Federal Aviation Administration: Air Traffic Organization Policy*, chap. 17. Traffic Management National, Center, and Terminal, Section 8.Monitor Alert Parameter, 2012.